Extinction of Methane Diffusion Flames Enriched by Hydrogen

Fernando F. Fachini
Instituto Nacional de Pesquisas Espaciais-INPE
fachini@lcp.inpe.br

Abstract. *This work is an extension of previous analysis (1) which has studied the influence of hydrogen in the methane diffusion flames. In this paper the aim is to determine the stable condition for methane diffusion flames enriched by hydrogen in different levels of flame stretch The stretch on the flame is provided by the flow field imposed by two opposed streams, one of them is constituted by mixtures of hydrogen, methane and nitrogen and the other is constituted by air. The flow field conditions correspond to fuel stream velocities in the range* 0.1 *to* $4.0\ m/s$*, which are chosen to compare the results of the present analysis to those from the n-heptane diffusion flame. The result presentation follows the flamelet model, the flame properties are presented as a function of the scalar dissipation* $\chi = 2(\lambda/\rho c_p)(dZ/dx)^2$*, whose unit is* s^{-1}*; Z is the mixture fraction. The reciprocal of scalar dissipation* χ^{-1} *at the flame is a measure of the residence time of the reacting substances inside the flame. The results pointed out that methane diffusion flame without and with hydrogen is not strongly influenced by stretch. For mixtures with high hydrogen concentration, this influence is even smaller. For a fixed fuel mixture concentration (*$Y_{CH4} + Y_{H2}$*), the flame temperature increases with the increase of the hydrogen mass fraction as a consequence, mainly, of the increase of the overall heat realised and, secondarily, of the reduction of the radiative energy losses via* CO_2 *radiation.*
Keywords: *bicomponent fuel, diffusion flame, Rate-Ratio Asymptotics, flame enriched by hydrogen*

1. Introduction

Hydrogen is pointed out as a fuel for the future because it does not pollute the environment. Meanwhile the conditions for the hydrogen usage as main fuel are not reached, it can be used in mixtures with hydrocarbons to reduce combustion emissions and to permit fossil fuels to be used for a longer period of time. The focus of this study is to analyse the influence of hydrogen in methane diffusion flames. In addition, methane is chosen as the main fuel because it is main substance in natural gas. Previous study (1) showed the influence of the concentrations of methane and hydrogen on the flame structure and flame temperature. In this work, the attention is on the fluid dynamical influence on the hydrogen-methane diffusion flames.

The idea of mixing a few quantity of hydrogen with other fuel, to improve the combustion as in energetic terms as in pollution terms, is not new. Scholte and Vaags (2; 3; 4) studied the effects of the hydrogen in the propagation of premixed flames. Recently, the mixture of fuel and hydrogen returned to the focus of attention due to the restrictions on the emissions into the ambient (5; 6; 7; 8; 9; 10).

The present analysis is performed asymptotically through the rate-ratio method (11). The flame structure described by this method shows the reaction zone embedded by a chemically inert, transport zone, whose order of magnitude is given by the combustion chamber characteristic length. The flow field in which the diffusion flame stabilises is imposed by two opposed streams (12) The reaction zone is composed by three layers and in each of them one or maximum two reactions are important. The chemical mechanism for the reaction is reduced from a reduced kinetic mechanism applying the steady state condition for some species and the equilibrium condition for some reactions (13). The simplified overall reaction mechanism for hydrocarbons includes a reduced hydrogen mechanism, then the addition of hydrogen to form a mixture does not demand an extension of the hydrocarbon chemical mechanism. By making use of this method, the influence of the stretch on the methane diffusion flames enriched by hydrogen is studied.

To avoid the large consume of CPU time in turbulent reacting flow simulations in certain conditions, the flow field and the chemistry are decoupled assuming the flame to be a infinitely thin frontier separating the fuel from the oxygen. The next approximation is to consider the flame as an ensemble of laminar diffusion flamelets (14). Because these flamelets are forced to move non stationarily by the turbulence, the flamelet flow configuration is represented well by the counterflow. Therefore, isolated flamelet can be studied numerically, experimentally and asymptoticly by the laminar counterflow diffusion flames, in which are included the reduced, simplified and full kinetic mechanisms. The results containing the chemistry are used to form libraries, which are consulted at each time step by the code simulating the turbulent reacting flow to determine the state of each flamelet (extinguished or burning). The analysis in the present work can be used in this way.

2. Simplified Overall Reaction Mechanism

Since this work is only an extension of previous analysis (1), the problem formulation is the same of that analysis; thus, its detailed presentation is unnecessary. Some parts of the formulation are exposed to help in the introduction of the paper.

The oxidation of methane and hydrogen is described by the following four-step chemical-kinetic mechanism

$$\begin{array}{lllllllll} CH_4 & + & 2H & + & H_2O & \rightleftharpoons & CO & + & 4H_2 & I' \\ CO & + & H_2O & & & \rightleftharpoons & CO_2 & + & H_2 & II' \\ 2H & + & M & & & \rightleftharpoons & H_2 & + & M & III' \\ O_2 & + & 3H_2 & & & \rightleftharpoons & 2H_2O & + & 2H & IV' \end{array} \tag{1}$$

Global reaction I' is chain-breaking and represents the reactions between the fuel and the radicals which form CO and H_2. Global reaction II' represents the oxidation of CO to form the final product, CO_2. Global reaction III' represents the three-body recombination steps and is also responsible for a major fraction of heat released in the flame. Global reaction IV' represents the reaction of O_2 with radicals and the formation of H_2O; it comprises the chain-branching steps.

The global reactions I' to IV' were determined from the simplified chemical-kinetic mechanism for methane shown in (13). In addition, the principal reaction rates for the these global reactions are given in terms of the elementary reactions (Table 1) according to

$$\begin{array}{lcl} w'_{I'} & = & w_{11f} \\ w'_{II'} & = & w_{9f} - w_{9b} \\ w'_{III'} & = & w_5 \\ w'_{IV'} & = & w_{1f} - w_{1b} \end{array} \tag{2}$$

The reaction rate coefficient k_i of the elementary reaction i, calculated using the expression $k_i = B_i T^{\alpha_i} exp[-E_i/(\bar{R}T)]$, in which T denotes the temperature, $\bar{R}$ is the universal gas constant, are given in the table 1.

Table 1. The main reactions of the chemical kinetic mechanism for methane oxidation[a]. Note that E_i is kJ/mol and B_i is such that w_i is given by mol/s.

$Number$	$Reaction$	B_i	α_i	E_i
$1f$	$O_2 + H \rightarrow OH + O$	2.000×10^{14}	0.00	70.338
$1b$	$OH + O \rightarrow O_2 + H$	1.575×10^{13}	0.00	2.888
$2f$	$H_2 + O \rightarrow OH + H$	1.800×10^{10}	1.00	36.952
$2b$	$OH + H \rightarrow H_2 + O$	8.000×10^{9}	1.00	28.302
$3f$	$H_2 + OH \rightarrow H_2O + H$	1.170×10^{9}	1.30	15.181
$3b$	$H_2O + H \rightarrow H_2 + OH$	5.090×10^{9}	1.30	77.824
$4f$	$OH + OH \rightarrow H_2O + O$	6.000×10^{8}	1.30	0
$4b$	$H_2O + O \rightarrow OH + OH$	5.900×10^{9}	1.30	71.297
5	$H + O_2 + M \rightarrow HO_2 + M$	2.300×10^{18}	-0.80	0
6	$HO_2 + H \rightarrow OH + OH$	1.500×10^{14}	0.00	4.203
7	$HO_2 + H \rightarrow H_2 + O_2$	2.500×10^{13}	0.00	2.930
8	$HO_2 + H \rightarrow H_2O + O$	3.000×10^{13}	0.00	7.200
$9f$	$CO + OH \rightarrow CO_2 + H$	4.400×10^{6}	1.50	-3.100
$9b$	$CO_2 + H \rightarrow CO + OH$	4.960×10^{8}	1.50	89.710
$11f$	$CH_4 + H \rightarrow H_2 + CH_3$	2.200×10^{4}	3.00	36.600
$11b$	$H_2 + CH3 \rightarrow CH4 + H$	8.830×10^{2}	3.00	33.530
12	$CH_4 + OH \rightarrow H_2O + CH_3$	1.600×10^{6}	2.10	10.300
13	$CH_3 + O \rightarrow CH_2O + H$	7.000×10^{13}	0.00	0.000
17	$CH_2O + H \rightarrow CHO + H_2$	2.500×10^{13}	0.00	16.700
18	$CH_2O + OH \rightarrow CHO + H_2O$	3.000×10^{13}	0.00	5.000
19	$CHO + H \rightarrow CO + H_2$	2.000×10^{4}	0.00	0.000
20	$CHO + OH \rightarrow CO + H_2O$	1.000×10^{4}	0.00	0.000
21	$CHO + O_2 \rightarrow CO + HO_2$	3.000×10^{2}	0.00	0.000
22	$CHO + M \rightarrow CO + H + M$	7.100×10^{4}	0.00	70.300

[a] (15).

In order to simplify the analysis, it is considered that the radicals O and OH are in steady-state. In addition, reactions 2 and 3 is considered in partial equilibrium.

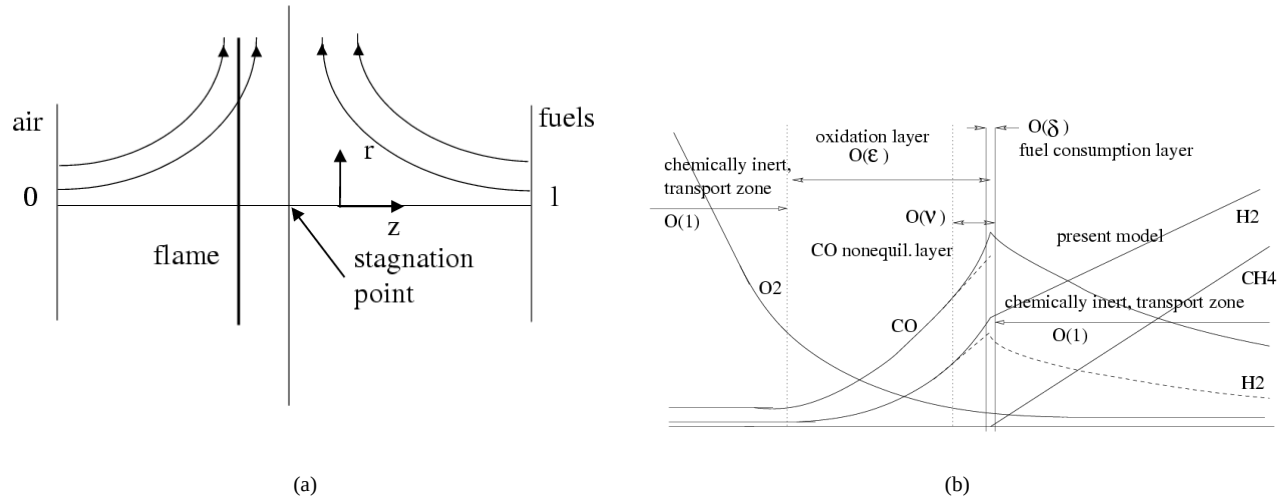

(a) (b)

Figure 1. Schematic pictures for a) outer and b) inner zones; the thickness of each layer inside inner zone satisfies the condition $\delta \ll \nu \ll \varepsilon \ll 1$.

3. Asymptotic Analysis

The asymptotic procedure is valid in the limit of large values for the Damkohler numbers (ratio of the flow characteristic time to the chemical time) of the reactions I, II, III and IV. Under this condition, the reaction zone (inner zone)is much thinner than the chemically inert, transport zone (outer zone). As a result, the outer zone can be described without detailed information of the reaction zone, except the jump conditions in the heat and mass fluxes through it. In terms of outer zone variables, the flame is seen as a discontinuity in the fluxes. These H_2O and CO_2 concentrations, flux continuities as well as the position and temperature of the flame are the outer zone properties necessary to perform the inner zone analysis.

3.1 Outer Zone

To present the results of this work in a form to be used in flamelet model, the geometry chosen for the outer structure of the diffusion flame is two opposing streams of air and a mixture of methane, hydrogen and nitrogen (Fig. 1.a).

In the counterflow configuration, the flame is established within the (viscous) mixing layer. In addition, the flame position in the viscous layer is imposed by the combustion conditions, such as oxygen concentration and fuel type and concentrations. Due to the flow field configuration, the flame suffers stretch; by increasing the velocity of the streams, increases the flame stretch. The stretch is the process responsible for the flame extinction in high stream velocities (or high scalar dissipation χ) (15; 16; 17). Besides, in flame with a large production of CO_2, extinction occurs for low stream velocity caused by the radiative heat losses (17).

The multicomponent fuel diffusion flame analysis presented in this work will be proceeded by having no restriction neither on the Lewis number nor on the heat transfer from the flame (12).

The counterflow configuration is characterised by the distance between the two nozzles l, the density of the air at the air nozzle ρ_1, and the density of the fuels at the fuel nozzle ρ_2. The concentration of the fuel mixture changes with addition of nitrogen, hence the fuel fluxes, $d_F,\ d_{H2}$, as well as the oxygen, d_{O_2}, change with the concentration at the nozzles and with the stream velocity.

3.2 Inner Zone

In the oxidation layer (Fig. 1.b), reaction II is much faster than reaction III and the reaction I is negligible because the fuel concentration is zero (15; 18; 19). Since, the reaction II is too fast, it is possible to consider it in partial equilibrium. Imposing these conditions in the species conservation equation for the H_2 and solving it with proper boundary conditions to match with solution of chemically inert, transport zone in the oxygen side of the flame and to match with the solution of the CO non-equilibrium layer, the following expression can be found for the oxidation layer thickness (1)

$$\varepsilon^4 D_{III} = 1 \tag{3}$$

$$D_{III} \equiv \left[\frac{L^2\rho_2^2}{D_{\theta,2}W_{N_2}}\right]\left[\frac{k_5 C_M K_1^{1/2}K_2^{1/2}K_3 a^{1/2} Le_{H_2}^{3/2} Le_{O_2}^{3/2}}{\theta_f^{m+2} X_{H_2O,f}}\left(\frac{d_{O_2}}{L_{O_2}}\right)^2\right] \tag{4}$$

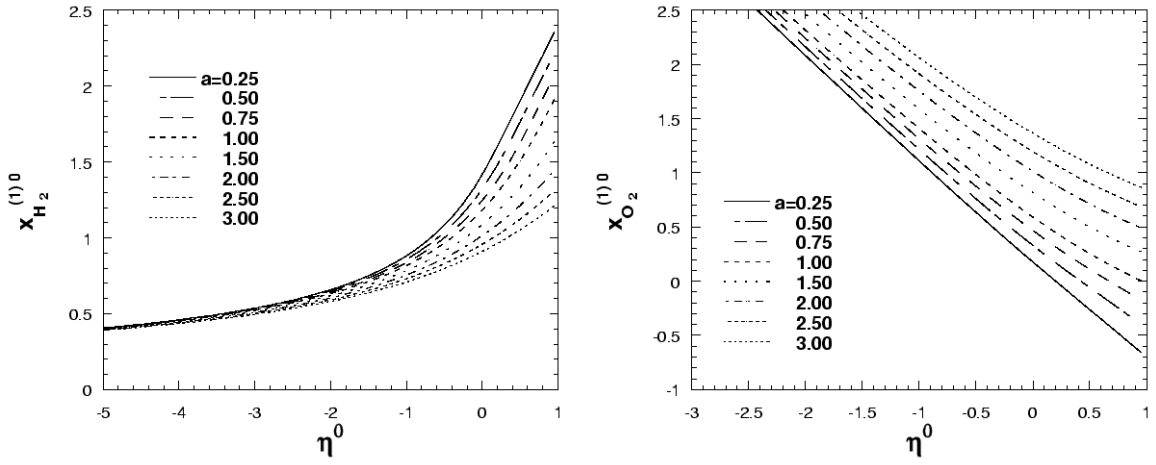

(a) (b)

Figure 2. The hydrogen concentration $x^{(1)0}_{H_2}$ and oxygen concentration $x^{(1)0}_{O_2}$ at the border of the flame $\eta = \eta^0$. The plots are obtained by proper value of the parameter a.

where D_θ is the thermal diffusivity, W_i is the molecular weight of species i, k_i is the reaction rate constant of reaction i given by Table 1, K_i is equilibrium constant of species i, $X_i \equiv Y_i/W_i$ and $\theta_f = T_f/T_2$ is the non dimensional flame temperature. The parameter a is the ratio of fuel fluxes to oxygen flux, already included the hydrogen flux to the flame.

Concentrations of H_2 and O_2 at the fuel consumption layer, $z = z_0$ are determined in the oxidation layer analysis and they are employed to solve the problem. Figure (2) shows the concentrations of hydrogen and oxygen, $x^{(1)0}_{H_2} = x^{(1)}_{H_2}(\eta^0)$ and $x^{(1)0}_{O_2} = x^{(1)}_{O_2}(\eta^0)$, for some values of the parameter a (1). It is apparent from this figure that $x^{(1)0}_{O_2}$ curves for $a < 1$ cross the limit of zero oxygen concentration, an unreal result. This means that the flame can not be sustained for those conditions.

In the non-equilibrium layer (Fig. 1.b), reaction II is not in partial equilibrium. The location of this layer is around the fuel consumption layer z^0, whose temperature is θ^0. As seeing in Fig. 1.b, variations of the order ν around z^0 causes variations in the properties $X_{H_2},\ X_{O_2},\ X_{CO}$ of the order ν. From the analysis of this layer, the thickness ν is specified

$$\nu^2 D_{II} \frac{(1+\beta)^3}{(1-\beta)} = 1 \tag{5}$$

and the definitions of D_{II} and β are

$$D_{II} \equiv \frac{L^2\rho_2^2}{D_{\theta,2}W_{N_2}} \frac{k_{9f}K_1^{0\,1/2}K_2^{0\,1/2}X_{H_2}^{0\,1/2}X_{O_2}^{0\,1/2}Le_{CO}}{\theta^{0\,m+2}}, \quad \beta \equiv \frac{Le_{H_2}K_3X_{CO_2}}{Le_{CO}K_9X_{H_2O}} \tag{6}$$

In the fuel consumption layer (Fig. 1.b), only reaction I is fast enough to occur within the thin layer of thickness δ. The fuel conservation equation with the boundary conditions takes a form that permits the integration. The results for the integration leads to

$$D_I\delta^2 = 15/8 \tag{7}$$

where

$$\delta = \frac{2k_{1f}X^0_{O_2}}{k_{11f}L_FA_F^{(3)}}, \quad D_I \equiv \frac{L^2\rho_2^2}{D_{\theta,2}W_{N_2}} \frac{k_{11f}K_1^{0\,1/2}K_2^{0\,1/2}K_3^0}{\theta^{0\,m+2}} \frac{X_{H_2}^{0\,3/2}X_{O_2}^{0\,1/2}}{X^0_{H_2O}}Le_F \tag{8}$$

4. Results and Comments

The results presented in this section are based on calculations performed for fixed values of $l = 0.02m$, $\rho_1v_1 = \rho_2v_2$, $0.1 \le v_2 \le 4(m/s)$, $m = 0.5$, $T_1 = T_2 = 390K$, $c_p = 1200J/(Kg.K)$ and $\lambda_2 = 0.035(J/m.K.s)$. Lewis numbers are $Le_F = 0.60$, $Le_{H_2} = 0.30$, $Le_{O_2} = 1.11$, $Le_{CO} = 1.10$, $Le_{CO_2} = 1.39$, $Le_{H_2O} = 0.85$. The presented cases correspond to five hydrogen concentrations, $Y_{H_2} = 0.01,\ 0.02,\ 0.03,\ 0.04,\ 0.05$, for methane concentrations that satisfy $Y_F + Y_{H_2} = 1,\ 0.8,\ 0.6,\ 0.4$. For these conditions, the reciprocal scalar dissipation $\chi^{-1} = [2(\lambda/\rho c_p)(dZ/dx)^2]^{-1}$ ranges

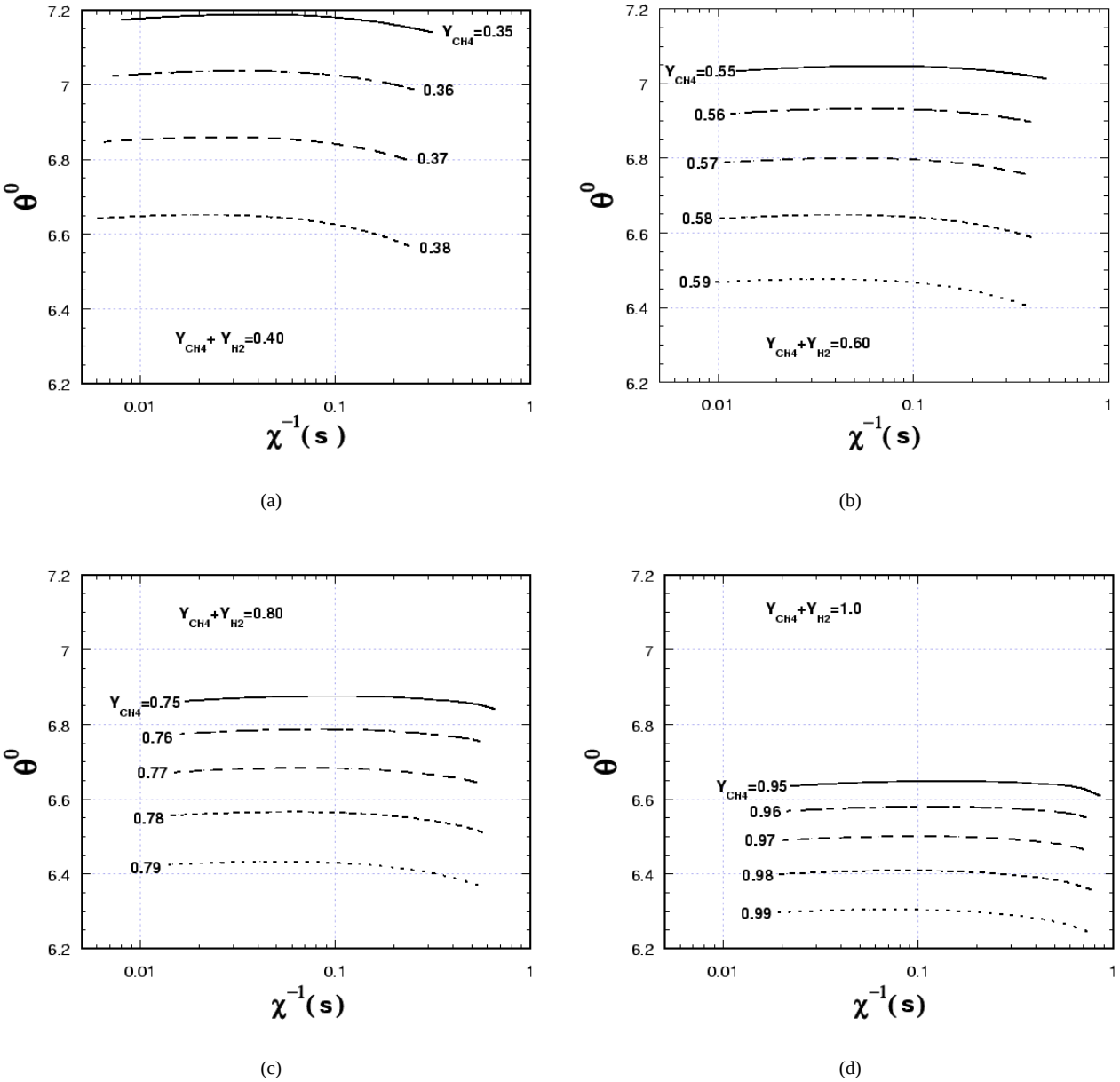

Figure 3. Flame temperature θ^0 as a function of the reciprocal scalar dissipation χ^{-1} for $Y_{H_2} = 0.01,\ 0.02,\ 0.03,\ 0.04,\ 0.05$ and $Y_F + Y_{H_2} = 1,\ 0.80,\ 0.6,\ 0.4$

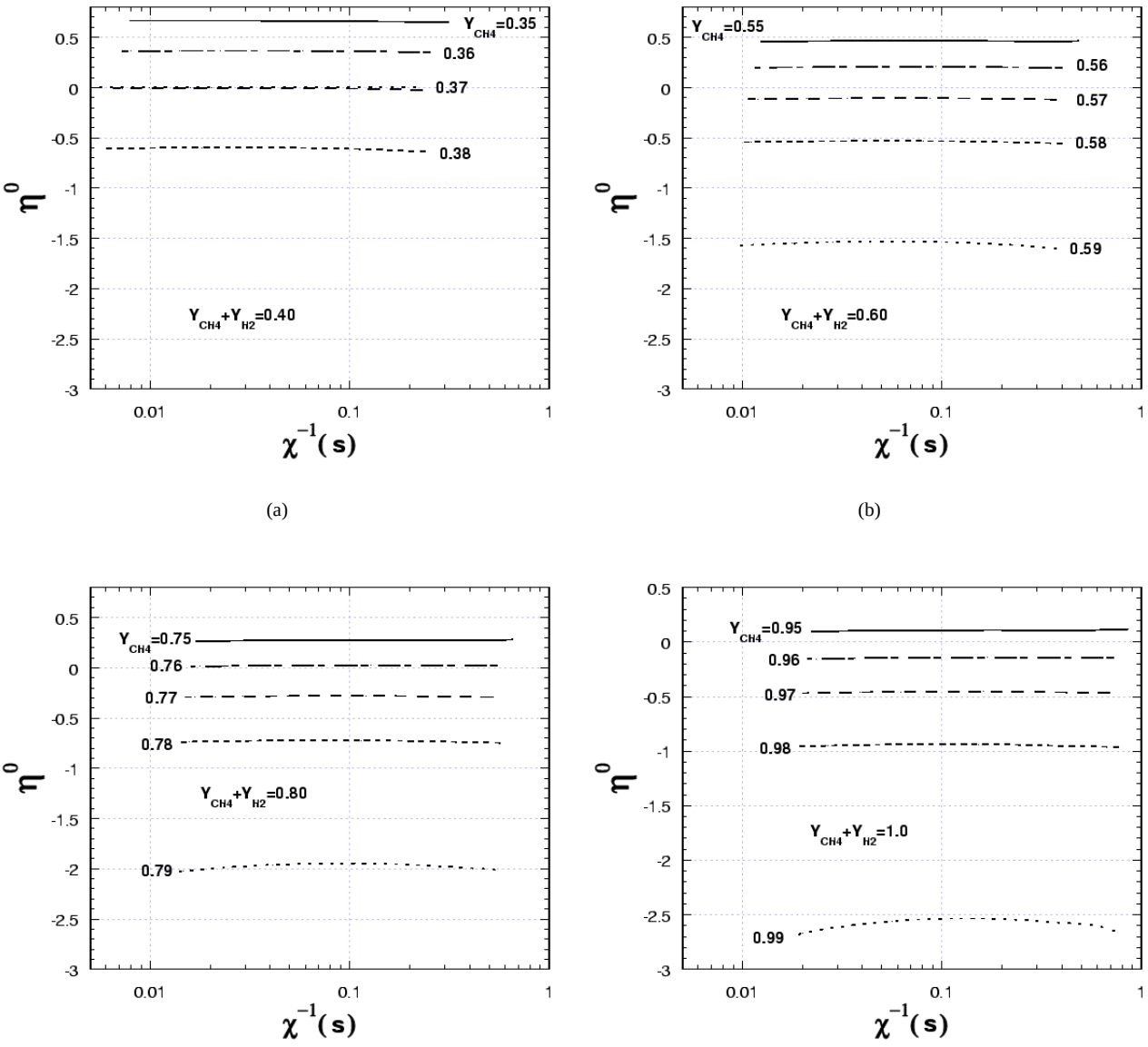

(a) (b)

(c) (d)

Figure 4. Fuel consumption layer position η^0 as a function of the reciprocal scalar dissipation χ^{-1} for $Y_{H_2} = 0.01,\ 0.02,\ 0.03,\ 0.04,\ 0.05$ and $Y_F + Y_{H_2} = 1,\ 0.80,\ 0.6,\ 0.4$

from 0.005 to 1. Although χ represents the stretch suffered by the flame, the figures are prepared using the reciprocal scalar dissipation χ^{-1} to depict the plots as a function of the residence time of the reacting substances inside the flame.

In fact, the variation of the stretch on the transport and reaction zones can be interpreted as a change in the hot gases volume around the flame. Since, from this volume comes out the thermal radiation mainly by the CO_2 band, an increase in the stretch causes a reduction of that volume and consequently a decrease in the radiative energy losses. In contrast, an increase in the stretch produces a decrease in the flame thickness and, thereby, an increase in the leakage of reactants through the flame.

Figure 3 displays the variation of the flame temperature θ^0 as function of the χ^{-1}. Except for the case $Y_F = 0.39$ and $Y_{H_2} = 0.01$ that is not shown because the flame does not find condition to be stable (extinction), the diffusion flame is stable in all cases exhibited. Although the variation of the flame temperature θ^0 with reciprocal scalar dissipation χ^{-1} is not important to produce extinction in the range $0.005 \leq \chi^{-1} \leq 1$, as was observed for the n-heptane diffusion flame (17). Even so, the cases with low methane concentration show the largest variation. This result is explained by the control of the H_2 reaction on the flame. Increasing H_2 concentration or reducing CH_4 concentration, the flame becomes more insensitive to the stretch because the H_2 reaction is not so dependent on the temperature as CH_4 reaction is. As expected, the influence of hydrogen on the flame temperature θ^0 is more evident for the cases with low methane concentration; compare the two extreme cases $Y_F + Y_{H_2} = 1,\ 0.4$.

CO_2 is the main responsible for the radiative energy losses. Consequently, the small formation of CO_2 in the oxidation of the methane leads to low radiative energy losses. Therefore, the variation of the flame temperature θ^0 with stretch (or reciprocal scalar dissipation) is small compared to heavier hydrocarbon (17). The low radiative energy losses for methane flames in conditions represented by $0.1 < \chi^{-1} < 1$ (large hot gases volume) does not permit the extinction of the flame.

In addition, since the presence of hydrogen in the mixture reduces the CO_2 concentration in methane or in other hydrocarbon diffusion flames, these flame becomes more stable in the regime $0.1 < \chi^{-1} < 1$.

A reduction of the value of χ^{-1} leads to a decrease in the hot gases volume around the flame, and, thereby, causes the reduction of the radiative energy losses. However, the reduction of χ^{-1} makes the residence time for the reactants inside the flame to become short and, thereby, part of the reactants leak by the flame. A consequence of the leakage is the reduction in the flame temperature. In the case of methane diffusion flames, the reactions controlling the fuel oxidation is fast enough to be practically insensitive to the stretch corresponding to the range $0.005 \leq \chi^{-1} \leq 0.1$. This methane chemical reaction characteristic guarantees that methane diffusion flames are stable under conditions that other hydrocarbon diffusion flames would be extinguished, like in the case of the n-heptane (17).

Figure 4 shows the fuel consumption layer position η^0 as a function of χ^{-1}. all cases, except the case $Y_F = 0.99$ and $Y_{H_2} = 0.01$, η^0 can be considered a constant for $0.005 < \chi^{-1} < 1$. The main effect on the η^0 is caused by the composition of the mixture fuel. The results confirm the fact that hydrocarbon diffusion flames take place in the oxygen side of the Burke-Schumann flame, $\eta^0 < 0$. However, there are mixtures for methane and hydrogen that $\eta^0 > 0$, indicating the strong influence of the hydrogen in the flame position.

5. Conclusion

This work analyses the structure and extinction of methane counterflow diffusion flames enriched by hydrogen. The presence of hydrogen causes an increase in the flame temperature due to the increase of the overall heat combustion and to the decrease of the radiative energy losses via reduction of the CO_2 concentration. Another effect of the hydrogen is to establish the flame in the fuel side of the Burke-Schumann flame. Flame extinction is observed only for the lowest concentration for the mixture ($Y_{CH_4} = 0.39,\ Y_{H_2} = 0.01$).

Acknowledgements This work was in part supported by the Conselho Nacional de Desenvolvimento Científico e Tecnológico - CNPq under the Grant 302801/03-0 and by the Fundação de Amparo à Pesquisa do Estado de São Paulo - FAPESP under the Grants 00/08997-4.

References

F. Fachini, Methane-hydrogen diffusion flames: Rate-ratio asymptotic., Proc. 10th Brazilian Congress of Thermal Engineering and Sciences, Nov.30th - Dec.3, 2004.

T. G. Scholte, P. B. Vaags, Burning velocities of mixtures of hydrogen, carbon monoxide and methane with air, Combust. Flame 3 (1959) 511–524.

T. G. Scholte, P. B. Vaags, The burning velocity of hydrogen-air and mixtures of some hydrocarbons with air, Combust. Flame 3 (1959) 495–501.

T. G. Scholte, P. B. Vaags, The influence of small quantities of hydrogen and hydrogen compounds on the burning velocity of carbon monoxide-air flames, Combust. Flame 3 (1959) 503–510.

R. Cheng, A. Oppenheim, Autoignition in methane hydrogen mixtures, Combust. Flame 58 (1984) 125–139.

B. E. Milton, J. C. Keck, Laminar burning velocities in stoichiometric hydrogen and hydrogen hydrocarbon-gas mixtures, Combust. Flame 58 (1984) 13–22.

E. Sher, S. Refael, A simplified reaction scheme for the combustion of hydrogen enriched methane air flame, Combust. Sci. Technol. 59 (1988) 371–389.

S. Refael, E. Sher, Reaction-kinetic of hydrogen-enriched methane air and propane air flames, Combust. Flame 78 (1989) 326–338.

S. Bell, M. Gupta, Extension of the lean operating limit for natural gas fueling of a sparked ignited engine using hydrogen blending, Combust. Sci. Technol. 123 (1997) 23–48.

G. S. Jackson, R. Sai, J. M. Plaia, C. M. Boggs, K. T. Kiger, Influence of h2 on the response of lean premixed ch4 flames to high strained flow, Combust. Flame 132 (2003) 503–511.

N. Peters, F. A. Williams, The asymptotic structure of stoichiometric methane-air flames, Combust. Flame 68 (1987) 185–207.

F. Fachini, N-fuels diffusion flame: Counterflow configuration, Proc. 16th Brazilian Congress of Mechanical Engineering, Nov.26th - 29th (2001) 171–177.

N. Peters, Numerical simulation of combustion phenomena (r. glowinski, b. larroutarou, r. teman, eds).

N. Peters, Laminar diffusion flamelet models in non-premixed turbulent combustion, Prog. Energy Combust. Sci. 10 (1984) 319–339.

K. Seshadri, N. Peters, Asymptotic structure and extinction of methane-air diffusion flames, Combust. Flame 73 (1988) 23–44.

B. Yang, K. Seshadri, Asymptotic analysis of the structure of nonpremixed methane air flames using reduced chemistry, Combust. Sci. Technol. 88 (1992) 115–132.

F. F. Fachini, K. Seshadri, Rate-ratio asymptotic analysis of nonpremixed n-heptane flames, Combust. Sci. Technol. 175 (2003) 125–155.

J. Card, F. Williams, Asymptotic analisys of the structure and extinction of spherically symmetrical n-heptane diffusion flames, Combust. Sci. Techn. 84 (1992) 91–119.

J. Card, F. Williams, Asymptotic analisys with reduced chemistry for the burning of n-heptane droplets, Combust. Flame 91 (1992) 187–199.